MOLECULAR AND CELLULAR BIOLOGY, Feb. 2009, p. 1083–1094 Vol. 29, No. 4
0270-7306/09/$08.00+0 doi:10.1128/MCB.01163-08

Deficiency of the Tetraspanin CD63 Associated with Kidney Pathology but Normal Lysosomal Function▽

Jenny Schröder,[1] Renate Lüllmann-Rauch,[2] Nina Himmerkus,[3] Irina Pleines,[4] Bernhard Nieswandt,[4] Zane Orinska,[5] Friedrich Koch-Nolte,[6] Bernd Schröder,[1] Markus Bleich,[3] and Paul Saftig[1]*

Biochemisches Institut, Christian-Albrechts Universität Kiel, Otto-Hahn-Platz 9, D-24118 Kiel, Germany[1]; Anatomisches Institut, Christian-Albrechts Universität Kiel, Otto-Hahn-Platz 8, D-24118 Kiel, Germany[2]; Physiologisches Institut, Christian-Albrechts Universität Kiel, Hermann-Rodewaldstr. 5, D-24118 Kiel, Germany[3]; Rudolf Virchow Center, DFG Research Center for Experimental Biomedicine, Zinklesweg 10, D-97078 Würzburg, Germany[4]; Forschungszentrum Borstel, Abteilung Immunologie und Zellbiologie, Parkallee 22, D-23845 Borstel, Germany[5]; and Institut für Immunologie, Universitätsklinikum Eppendorf, Martinistr. 52, D-20246 Hamburg, Germany[6]

Received 23 July 2008/Returned for modification 24 October 2008/Accepted 2 December 2008

CD63 is a member of the tetraspanin superfamily that constitutes a main component of the lysosomal membrane. In mice, two CD63 gene loci are present, with only one of these two being functional. We generated and analyzed mice deficient for active CD63. Disruption of CD63 results in a complete loss of CD63 protein expression. Despite its abundance in late endosomes/lysosomes, the lack of CD63 does not cause obvious endosomal/lysosomal abnormalities. CD63 knockout mice are viable and fertile without gross morphological abnormalities in the majority of tissues. No alterations in the populations of immune cells and only minor differences in platelet function were observed. This suggests that the lack of CD63 could be successfully compensated for, most likely by other tetraspanins. However, CD63 deficiency leads to an altered water balance. CD63 knockout mice show an increased urinary flow, water intake, reduced urine osmolality, and a higher fecal water content. In principle cells of the collecting duct of CD63-deficient mice, abnormal intracellular lamellar inclusions were observed. This indicates that the sorting of apical transport proteins might be impaired in these cells. CD63 knockout mice provide an important tool for analyzing the various postulated functions of CD63 in vivo.

CD63, also called lysosomal integral membrane protein LIMP-1 (21), belongs to the family of tetraspanins (also known as the transmembrane 4 [TM4] superfamily, TM4SF, 4TM, and the tetraspan family). This family is composed of 33 members in mammals, spanning the membrane four times and forming a small and a large extracellular loop (7, 76). Tetraspanins are present in the plasma membrane as well as in the membranes of a variety of subcellular compartments, like multivesicular bodies (for a review, see reference 7). Conserved polar amino acid residues in the transmembrane domains probably mediate stable protein assembly through their interaction with polar residues of other transmembrane helices (46). Many tetraspanins have the tendency to associate with other molecules, such as proteins of the immunoglobulin superfamily, proteoglycans, complement regulatory proteins, growth factors, growth factor receptors, signaling enzymes, integrins, and other tetraspanins (28, 49). These interactions led to the proposal that tetraspanins have a role as "molecular facilitators." Tetraspanins group specific cell surface proteins and thereby increase the formation and stability of functional signaling complexes. Such complexes are involved in diverse cellular processes, such as cell activation, adhesion, motility, differentiation, and malignancy (29, 49, 86).

CD63 is an exceptional tetraspanin since at steady state it is usually found as a heavily glycosylated protein in late endosomes/lysosomes (7). Using a tyrosine motif in the cytoplasmic carboxy-terminal tail (Tyr 235) and interaction with adaptor protein complex 3, it is directed to lysosomes (67). CD63 is also present in various lysosome-related vesicles of different leukocytes, like the α-granules of megakaryocytes (27), the cytotoxic granules of T lymphocytes (61), the crystalloid granules of eosinophils (50), the secretory granules of basophilic granulocytes (59), and mast cells (20). CD63 is also expressed in the Weibel-Palade bodies of the vascular endothelium (42) and in the dense granules and α-granules of platelets (27, 58). These granules are translocated to the surface after cell activation, transferring CD63 into the plasma membrane. This surface expression of CD63 in platelets serves as an important diagnostic activation marker (39, 64).

Surface-expressed CD63 may be involved in different adhesion processes. Monoclonal anti-human CD63 (anti-hCD63) antibodies enhanced the adhesion and spreading of monocytic cells on serum-coated plastic (44). On the other hand, an impairment of adhesion of neutrophilic granulocytes to lipopolysaccharide- or thrombin-pretreated endothelium was observed (79). Additionally, another antibody induced rapid internalization of hCD63, which was accompanied by an increased migration ability among dendritic cells in vitro (52). A role for CD63 in platelet adhesion and spreading has also been described (35). CD63-mediated adhesion events may involve integrins. CD63 associates with β1 integrins in human melanoma cells (65), the α^3/β_1 complex in lymphocytes and

* Corresponding author. Mailing address: Biochemisches Institut, Christian-Albrechts Universität Kiel, Otto-Hahn-Platz 9, D-24118 Kiel, Germany. Phone: 49/(0)431-8802216. Fax: 49/(0)431-8802238. E-mail: psaftig@biochem.uni-kiel.de.

▽ Published ahead of print on 15 December 2008.

melanoma cells (6, 9), the α^4/β_1 complex in T lymphoblasts (51), and the α^6/β_1 complex in various cell lines (6).

In basophilic granulocytes and mast cells, CD63 interacts with the high-affinity immunoglobulin E (IgE) receptor (FcεRI) (38). Therefore, CD63 might be involved in mediating FcεRI signals that lead to a release of inflammatory mediators. These mediators might then cause allergic reactions (45). Similarly, in cytotoxic T cells, CD63 was found in a complex with the T-cell receptor. A CD63 specific monoclonal antibody triggered strong T-cell activation, which is characterized by pronounced induction of proliferation, strong interleukin-2 production, and enhanced T-cell responsiveness to restimulation (62).

The importance of CD63 in cell signaling is highlighted by the observation that CD63 associates with a 55-kDa type II phosphoinositide 4 kinase in intracellular vesicles as well as in focal adhesions at the plasma membrane (8, 85). The latter interaction also involves CD81 and the integrin α^3/β_1 (8).

CD63 is also associated with intracellular major histocompatibility complex class II molecules in immature dendritic cells and B lymphocytes (17, 18, 26). CD63 surface expression is increased in neutrophils undergoing apoptosis due either to aging or to stimulation of the Fas receptor (5). CD63 is expressed strongly during the early stages of tumor progression of melanomas and was accordingly called melanoma-associated antigen (ME491) (1, 2, 73). It is also expressed in other types of tumors, such as neuroendocrine tumors, adenocarcinomas, and colorectal carcinomas (2, 19).

Based on experiments using monoclonal antibodies against CD63, a possible role for CD63 in human immunodeficiency virus type 1 infection of macrophages was suggested. CD63 might inhibit human immunodeficiency virus type 1 infection in a step after fusion of the virus with the plasma membrane but prior to reverse transcription (82).

Despite the abundant data on the presumed role of CD63 in isolated cell types, its function in vivo remains largely unknown. To address this question, we have generated and characterized a CD63-deficient mouse strain. The phenotype of these mice suggests a redundant role for CD63 in development and distribution of immune system cells, very mild effects on platelet adhesion, and an important role in kidney physiology.

MATERIALS AND METHODS

Materials. Restriction enzymes and other reagents for molecular biology were purchased from Fermentas (Burlington, Canada). Primers were purchased from Sigma Aldrich (Steinheim, Germany). Protein standards were obtained from Invitrogen (Carlsbad, CA). The BCA protein assay kit and Western blotting reagents were purchased from Pierce (Rockford, IL) and Amersham (Little Chalfont, United Kingdom), respectively.

Expression plasmid generation. To generate the CD63 expression plasmid, total RNA of wild-type mouse embryonic fibroblasts (MEF) (C57/BL6J) was prepared using RNeasy columns from Qiagen (Hilden, Germany). mRNA was transcribed into cDNA by using the Omniscript reverse transcriptase system (Qiagen, Hilden, Germany). For amplication of the CD63 cDNA in a standard PCR, primers which generated EcoRI and BamHI restriction sites (underlined) were used (fw_Chrom10/18, 5′-TTGAATTCTTCCATGGCGGTGGAAGGAG GAATG-3′; and bw_Chrom10, 5′-TTGGATCCTTCCAGCCCTACATTACTT CATAGC-3′). For cloning of the CD63-related gene, DNA was isolated from wild-type MEF (C57Blc6) by using an InnuPrep DNA minikit (AJ Innuscreen; Jena, Germany). The CD63-related gene was amplified using the following primers: fw_Chrom10/18, 5′-TTGAATTCTTCCATGGCGGTGGAAGGAGG AATG-3′; and bw_Chrom18, 5′-TTGGATCCTTCCAGCCCTACATTACTTC ATGGC-3′. The resulting PCR products were subcloned into the pEGFP-C1 expression vector (Invitrogen, Carlsbad, CA). All recombinant sequences were determined to be free of PCR errors by nucleotide sequence analysis (MWG Biotech AG, Martinsried, Germany).

Generation of mutant mice. A λ-EMBL3-129SV mouse phage library from Stratagene, Inc. (La Jolla, CA) was screened with a partial cDNA of mouse CD63 comprising exons 2 to 5. The isolated mouse CD63 phage contained the murine CD63 (mCD63) gene comprising exons 1 to 6. HindIII-digested phage DNA comprising exons 1 to 4 of mouse CD63 was introduced in pBluescript KS (Stratagene, La Jolla, CA). The neo expression cassette (Stratagene, La Jolla, CA) was inserted by mutagenesis PCR as an XbaI fragment into an NheI restriction site introduced in the third codon (coding for valine) of exon 2 of the CD63 gene. The targeting vector was electroporated into the embryonic stem (ES) cell line E14 (32). The thymidine-kinase cassette at the 3′ end of exon 4 allowed negative selection by 25 μg/ml ganciclovir. G418-resistant colonies (335 μg/ml) were screened by Southern blot analysis of DNA digested with BglII, XbaI, or NheI. A HindIII/BamHI fragment was used as probe A. The mutated ES line was microinjected into blastocysts of C57BL/6J mice. Chimeric males were mated to C57BL/6J females. Mice were genotyped for the CD63 gene mutation by Southern blot analysis or by PCR analysis using a neo expression cassette-specific PCR (69) and an exon-specific PCR with primers (5′-GGAGA CGTGGGTCTGACCGCG-3′ and 5′-CCAGCTGCCTTCATCTCTGGT-3′) flanking exon 2.

Northern blot analysis and reverse transcriptase PCR (RT-PCR). RNA of kidney and MEF was prepared using RNeasy columns from Qiagen (Hilden, Germany).

For Northern blot analysis, a radioactive, mCD63 mRNA-specific hybridization probe was generated by amplification of a 368-bp fragment encompassing exons 2 to 5 of mCD63 cDNA, using the primers 5′-GCGGTGGAAGGAGGA ATGA-3′ and 5′-ATAGTGGCTGTTTTGTTGT-3′. A GAPDH (glyceraldehyde-3-phosphate dehydrogenase)-specific hybridization probe was generated by conventional PCR using the primers 5′-CGCATCTTCTTGTGCAGTGC-3′ and 5′-GGTGGTCCAGGGTTTCTTAC-3′.

For RT-PCR, 2 μg of total mRNA was used for cDNA synthesis, using the Omniscript reverse transcriptase system (Qiagen, Hilden, Germany) and the oligo(dT)15 primer (Promega, Madison, WI). For amplification of the CD63 or actin cDNA, specific primers were used in a standard PCR (30 s at 94°C, 120 s at 55°C, and 60 s at 72°C for 36 cycles, using primers CD63fw [5′-CGGTGGA AGGAGGAATGAAG-3′], CD63bw [5′-CTACATTACTTCATAGCCACTTC G-3′], ACTfw [5′-GACGAGGCCCAGAGCAAGAC-3′], and ACTbw [ATCTC CTTCTGCATCCTGTC-3′]).

Cell lines. MEF from CD63-deficient and wild-type mice were generated from E12.5 embryos according to reference 31. Primary cell lines between passages 3 and 6 were used for the experiments. Cells were transiently transfected using Fugene 6 (Roche, Mannheim, Germany).

Antibodies and antibody generation. The following antibodies were used: rat anti-mouse LAMP-1 (1D4B) and rat anti-mouse LAMP-2 (Abl93) (Developmental Studies Hybridoma Bank, Iowa City, IA), rabbit anti-mouse cathepsin D (sII9) (63), rabbit anti-mouse MPR-46 (MSC1) (40), and rabbit anti-rat MPR-300 (12).

Anti-mouse CD63 peptide antibodies were raised in specific pathogen-free rabbits at Eurogentec (Seraing, Belgium) against two peptides (C-ATILDKLQ KENN [amino acids {aa} 132 to 143 of mCD63] and CGNDFKESTIHTQG [aa 176 to 189 of mCD63]). The resulting antiserum was affinity purified over a mixture of ACH [N^{α}-(ε-aminocaproyl)-DL-homoarginin-hexylester]- and cyanogen bromide-Sepharose covalently coupled with the peptide encompassing aa 132 to 143.

Antisera raised against the native mCD63 protein were generated by cDNA immunization. A CD63 expression construct containing the CD63 DNA (chromosome 10) cloned into the BamHI and EcoRI restriction sites of the pcDNA3.1-Zeo(-) vector (Invitrogen, Carlsbad, CA) was conjugated to 1-μm gold particles (Bio-Rad), and rabbits were immunized by ballistic DNA immunization (pressure setting at 400 lb/in^2). Animals received four immunizations at three 6-week intervals, with eight shots of plasmid-conjugated gold particles (1 μg DNA/mg gold/shot). Serum samples were obtained at 10 days postimmunization (43). Horseradish peroxidase-conjugated secondary antibodies for immunoblotting were obtained from Sigma Chemical Co. (St. Louis, MO).

Immunocytochemistry. For immunostaining, cells were grown on glass coverslips, fixed in 4% paraformaldehyde in phosphate-buffered saline (PBS) for 20 min, and permeabilized with PBS-0.2% saponin. The primary and secondary antibodies were diluted in PBS-3% bovine serum albumin (BSA)-0.2% saponin and applied to the cells for 1 h. Alexa Fluor 488- or 594-conjugated antibodies were from Molecular Probes (Eugene, OR). Cells were embedded in Mowiol containing Dabco (Sigma Aldrich, Steinheim, Germany) as an antifading agent.

Photographs were taken using an Axiovert 200 M microscope equipped with an ApoTome for optical sectioning, using Axio Vision 4.6 software (Carl Zeiss, Jena, Germany).

Sodium dodecyl sulfate-polyacrylamide gel electrophoresis and immunoblotting. Peritoneal macrophages and polymorphonuclear leukocytes were isolated for 3 h and 96 h, respectively, after thioglycolat injection. Erythrocytes were removed from bone marrow and spleen preparations by incubation with erythrocyte lysis solution (155 mM NH_4Cl, 15 mM $KHCO_3$, 1 mM EDTA, pH 7.3). All cells were lysed and proteins solubilized in 0.1% Triton X-100–PBS supplemented with complete protease inhibitor cocktail (Roche, Mannheim, Germany). Lysates were purified by centrifugation, and proteins were deglycosylated overnight by incubation with recombinant *N*-glycosidase F (Roche, Mannheim, Germany) according to the manufacturer's instructions. Proteins (5 μg/lane) were separated by Laemmli sodium dodecyl sulfate-polyacrylamide gel electrophoresis and transferred to polyvinylidene fluoride membranes (Millipore Corp., Bedford, MA), using a semidry electroblotter (Bio-Rad, Hercules, CA). Immunoblots were blocked in 5% low fat milk powder in Tris-buffered saline containing 0.1% Tween 20 and then probed with a polyclonal rabbit anti-mouse CD63 antibody at a 1:400 dilution in 1% BSA–0.1% Tween 20–Tris-buffered saline, followed by an incubation in 0.1 μg/ml of an appropriate horseradish peroxidase-conjugated secondary IgG in 1% BSA. All blots were developed using an enhanced chemiluminescence detection system (Amersham, Little Chalfont, United Kingdom).

Histology. For conventional light and electron microscopic examination, four CD63-deficient mice (aged 14 months) and two age-matched wild-type mice were used. Tissues were perfused with glutaraldehyde (6% in PBS). Tissue blocks were processed for light and electron microscopic examination (embedding in araldite) according to routine procedures. Tissue blocks were rinsed in phosphate buffer, postfixed in OsO_4 for 2 h, and embedded in araldite according to routine procedures. For light microscopy, 1-μm semithin sections were stained with Toluidin blue. Ultrathin sections were contrasted with uranyl acetate and lead citrate and observed with a Zeiss EM 900 microscope.

Analysis of platelets. Mice were bled under ether anesthesia from the retroorbital plexus. Blood was collected in a tube containing 10% (vol/vol) 0.1 M sodium citrate or 7.5 U/ml heparin. Platelet-rich plasma was obtained by centrifugation at 300 × *g* for 10 min at room temperature. Murine platelets were prepared according to established protocols (57). Tail bleeding time was determined as described in reference 66. Adhesion under flow conditions (thrombus formation) was assessed as described previously (56). Aggregometry was performed as described in reference 66.

To analyze platelets by flow cytometry, heparinized whole-blood samples were diluted 1:30 in modified Tyrode's solution-HEPES buffer (134 mM NaCl, 0.34 mM NaH_2PO_4, 2.9 mM KCl, 12 mM $NaHCO_3$, 20 mM HEPES, 5 mM glucose, 1 mM $MgCl_2$, pH 6.6) and stained against the following surface glycoproteins (GPs) with the indicated antibodies (54, 55): rat anti-mouse GPVI (JAQ1), rat anti-mouse α2-integrin (Sam.G4), rat anti-mouse GPIIbIIIa (JON1), rat anti-mouse GPV (DOM1), rat anti-mouse GPIb (p0p4), rat anti-mouse GPIX (p0p6), rat anti-mouse CD9 (ULF1), and rat anti-mouse β1-integrin (9EG7; BD Pharmingen, Franklin Lakes, NJ).

To activate platelets, samples were stimulated with the indicated concentrations of ADP (Sigma Aldrich, Steinheim, Germany), U46619 (1 μM; Alexis Biochemicals, San Diego, CA), collagen-related peptide (CRP; a kind gift from Steve P. Watson, Department of Pharmacology, University of Oxford, United Kingdom), or thrombin (Roche, Mannheim, Germany) for 10 min at room temperature, stained against activated GPIIbIIIa (JON/A-PE) or P-selectin, and directly analyzed with a FACSCalibur (Becton Dickinson, Franklin Lakes, NJ).

Flow cytometry of leukocytes. Single-cell suspensions were prepared from the thymuses, spleens, bone marrow, and lymph nodes of 3-month and 12-month-old mice. Peritoneal cavity cells were obtained by peritoneal lavage with 0.9% NaCl solution. Red blood cells were lysed by a 12-min incubation in a hypotonic solution containing 155 mM NH_4Cl, 15 mM Na_2CO_3, and 1 mM EDTA (pH 7.3), followed by washing in PBS containing 2% newborn calf serum, 0.1% NaN_3, and 0.2 mM EDTA and staining with antibodies against cell surface molecules. For flow cytometric analysis, the indicated unlabeled, biotinylated, or phycoerythrin-, allophycocyanin-, or fluorescein isothiocyanate-conjugated antibodies against the following cell surface molecules were used: CD3ε (145-2C11), CD4 (RM4-5), CD8α (53-6.7), CD11b (M1/70), CD45R/B220 (RA3-6B2), CD49b (DX5), CD69 (H1.2F3), IgD (11-26c.2a), IgM (R6-60.2), and Gr1 (RB6-8C5) (all from BD Biosciences) and CD31 (390) and Ly-6C (HK1.4) (Southern Biotechnology). Biotinylated antibodies were visualized with fluorescein isothiocyanate- or allophycocyanin-conjugated (BD Pharmingen, Franklin Lakes, NJ) or phycoerythrin-conjugated (Biosource International, Camarillo, CA) streptavidin. In order to prevent unspecific binding, all samples were preincubated with Fc Block or unlabeled, isotype-matched unspecific antibodies (BD Pharmingen, Franklin Lakes, NJ). Samples were analyzed with a FACSCalibur flow cytometer (Becton Dickinson, Franklin Lakes, NJ) according to standard protocols. Gates on viable cells were set according to the exclusion of propidium iodide staining. Analysis of different cell populations in bone marrow according to CD31 and Ly-6C expression was performed as described in reference 14.

Metabolic analysis. For investigation of intake and excretion, 11- to 12-month-old female CD63-deficient mice and age- and sex-matched control animals were kept in mouse metabolic chambers (Harvard Apparatus, Holliston, MA) with free access to water and a conventional mouse diet (Ssniff, Soest, Germany). After 24 h, final blood samples were taken from the abdominal vein under short-term anesthesia with 2.5% Forene in 500 to 1,000 ml/min air (Abbott, Wiesbaden, Germany) (Dräger Vapor; Dräger, Lübeck, Germany), and mice were sacrificed. Urine osmolality was determined using a Fiske micro-osmometer (model 210; Fiske Associates, Norwood, MA). Urinary concentrations of Na^+, K^+, Cl^-, Ca^{2+}, urea, creatinine, and glucose were measured with a Roche Modular P analyzer (Roche Diagnostics, Germany). To determine the dry weight of feces, a defined portion was dried at 37°C until the weight remained constant.

Statistical analysis. Statistical analyses were performed by Student's *t* test.

RESULTS

The mouse genome contains two CD63 loci on chromosomes 10 and 18. Genetic localization of the murine homologue to hCD63 revealed two distinct loci in the mouse genome (25). The genuine CD63 locus was found on chromosome 10, but a CD63-related locus without any intronic sequences localized to chromosome 18. Alignment of both genes revealed five amino acid substitutions (Fig. 1A), including an exchange of tyrosine to histidine at position 235 in the cytoplasmic targeting motif. By use of in silico promoter analysis, a considerable promoter activity was found for the locus only on mouse chromosome 10 (data not shown). Consistently, the UniGene database (www.ncbi.nlm.nih.gov/unigene) contains 925 expressed sequence tags for the genuine CD63 locus (UGID:1414132) but only 7 expressed sequence tags for the chromosome 18 locus (UGID: 2026693). To further address the physiological role of the additional, presumably silent gene locus on chromosome 18, we transfected MEF with expression vectors encoding chromosome 10-associated enhanced green fluorescent protein (eGFP)-CD63 and chromosome 18-associated eGFP-CD63 (Fig. 1B). Whereas the protein encoded by the chromosome 10 gene localized as expected to lysosomes, the exogenous expression of the chromosome 18 gene led to a diffuse and mainly plasma membrane staining.

Targeting of the CD63 gene on the mouse chromosome 10 locus leads to loss of CD63 expression. A gene targeting vector was constructed to disrupt mouse CD63 (Fig. 2A), and homologous recombined ES cell clones were used to generate chimeras that transmitted the introduced mutation to their offspring (Fig. 2B). Northern blotting (Fig. 2C) and RT-PCR (Fig. 2D) demonstrated a complete absence of CD63 RNA in homozygous CD63-deficient mice. Since no functional antibodies against mouse CD63 were available, we generated polyclonal rabbit antibodies directed either against a synthetic peptide from the second large luminal domain or against the entire native protein by cDNA immunization. The anti-peptide antibody clearly detected deglycosylated mCD63 in immunoblot analyses (Fig. 2E, panel a) but reacted only weakly with the fully glycosylated protein (Fig. 2E, panel b). Note that the anti-peptide serum is directed against a sequence that is identical in the predicted products of the two loci. The finding that this serum did not show any detectable bands in various iso-

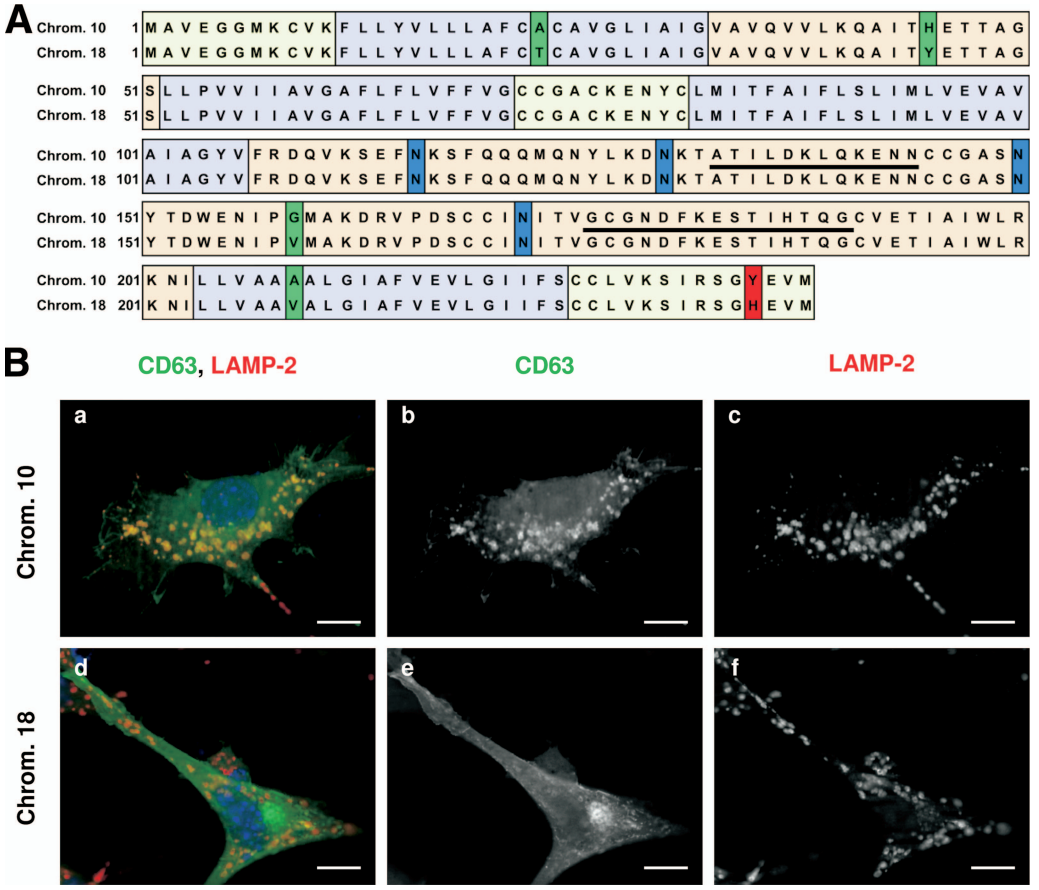

FIG. 1. Comparison between the CD63 gene and pseudogene. (A) Alignment of the mCD63 gene on chromosome (Chrom.) 10 and the pseudogene on chromosome 18. Red or green, amino acid substitutions; blue, N glycosylation sites (N-X-S/T); purple, transmembrane domains; yellow, cytoplasmic loops; orange, extracellular domains; black lines, synthetic peptides used for immunization (DNAstar software; DNASTAR, Inc., Madison, WI). (B) MEF were transfected with pEGFP-mCD63-C1-10 (chromosome 10, gene) (a to c) or with pEGFP-mCD63-C1-18 (chromosome 18, pseudogene) (d to f). Cells were costained against lysosome-associated membrane protein 1 (LAMP-1). The majority of CD63 is colocalizing with LAMP-2 in the lysosomal compartment, whereas the protein arising from the CD63 pseudogene is not localized to the lysosomal compartment. This can be explained by the Y-to-H mutation in the C-terminal sorting motif of the protein. (a, d) Merged (green, eGFP-CD63; red, LAMP-2); (b, e) eGFP-CD63; (c, g) LAMP-2. Scale bar = 10 μm.

lated CD63$^{-/-}$ cells (Fig. 2E) further underscores the lack of significant expression of the intronless locus on chromosome 18. These data were confirmed by immunocytochemical analysis of MEF with the rabbit antiserum directed against the native CD63 protein (Fig. 3A to F). The lack of the protein does not lead to any other marked morphological alterations of the late endosomal/lysosomal compartment, since normal distribution and staining with lysosomal markers were observed (Fig. 3G to L). Lysosomal enzyme activities, autophagic and phagocytic maturation, acidification, and endocytotic transport were also not found to be different when wild-type and CD63 knockout cells were compared (data not shown). The localization of mannose 6-phosphate receptors (MPR46 and MPR300) to the trans-Golgi network was also not affected by the CD63 deficiency (Fig. 3M to P), suggesting normal biosynthetic delivery of lysosomal hydrolases.

Homozygous CD63-deficient mice survive and are fertile; on first sight, they manifest no overt phenotypic abnormalities. A detailed fluorescence-activated cell sorting analysis of immune cells of the bone marrow, spleen, and lymph node did not reveal significant changes when cell distribution, cell numbers, and expression of specific cell surface molecules or activation markers were compared between wild-type and knockout mice (Table 1). Also, no differences in B-cell differentiation in the bone marrow or T-cell differentiation in the thymus were observed (data not shown).

Platelet function in CD63-deficient mice. CD63 is localized together with P-selectin in the α-granules of platelets, which translocate to the plasma membrane on activation. This led to an alternative CD63 nomenclature: granulophysin or platelet GP of 40 kDa (Pltgp40) (3, 27, 30, 34). A monoclonal antibody directed against the second, large extracellular loop of hCD63 impaired the spreading of platelets (35). CD63-deficient mice display normal numbers of platelets in peripheral blood (Fig. 4A), and the expression levels of prominent surface GPs, including GPIaIIa, GPIIbIIIa, GPIb-V-IX, and GPVI, as well as the tetraspanin CD9, are unaltered (data not shown). Activation of wild-type and mutant platelets by different agonists resulted in similar activations of GPIIbIIIa (as measured by the JON/A-PE antibody) (10) and surface exposure of P-se-

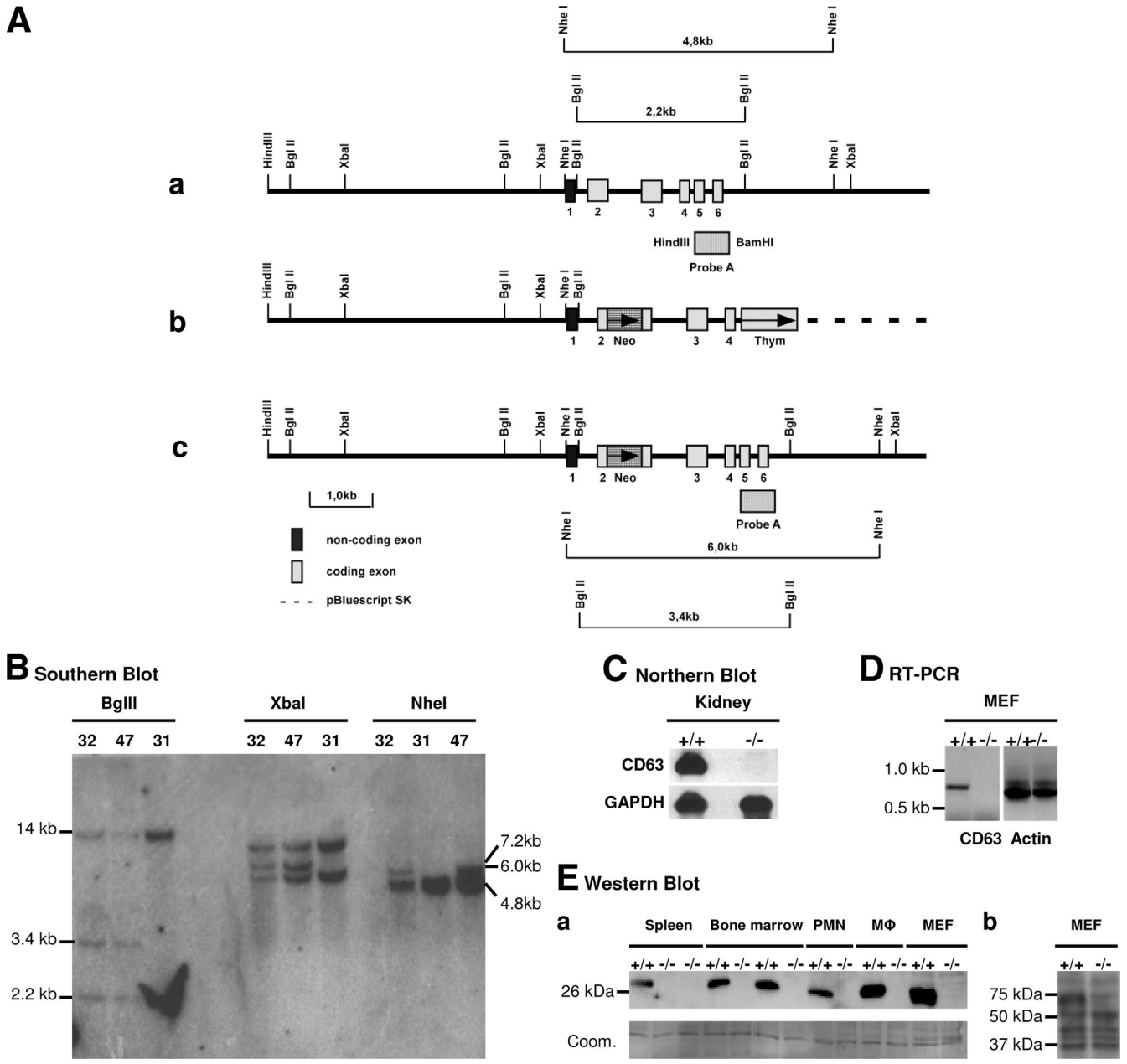

FIG. 2. Targeted disruption of the CD63 gene on mouse chromosome 10. (A) Strategy for the inactivation of the CD63 gene by homologous recombination in ES cells. (a) Partial structure of the genomic locus representing about 12 kb of the CD63 gene region. Coding exons are indicated by light gray boxes, noncoding exons by black boxes, and flanking introns by solid lines. Probe A denotes a DNA probe used for Southern blot analysis. (b) Targeting vector pBluescript KS-CD63-neo/TK, with about 7.4 kb homology to the CD63 gene locus. The neo cassette was inserted as an XbaI fragment into an NheI restriction site at Val3 introduced in exon 2 by mutagenesis PCR. (c) Predicted CD63 gene locus after homologous recombination. (B) Southern blot analysis of ES cell clones. Probe A was hybridized to BglII-, XbaI-, or NheI-digested genomic DNA from ES cell clones E32, E47, and E31. Additional 3.4-kb, 7.2-kb, and 6.0-kb DNA fragments, respectively, indicate a targeted allele. (C) Northern blot analysis of kidney and MEF cells. (D) RT-PCR analysis of CD63 expression. Total RNA was used for reverse transcription, followed by PCR amplification of the CD63 cDNA open reading frame. A 712-bp fragment is amplified in $CD63^{+/+}$ and is absent in CD63-deficient MEF. (E) Western blot analysis of CD63 expression using an antibody directed against a synthetic peptide from the second luminal loop E2 of mCD63. (a) Proteins in cell lysates derived from wild-type and CD63-deficient mice were deglycosylated using PNGase F. (Upper) Deglycosylated CD63 molecules were detected in $CD63^{+/+}$ cells and absent in CD63-deficient cells. PMN, polymorphonuclear leukocyte; MΦ, macrophage. (Lower) Coomassie staining of the membrane demonstrates equal protein loads. (b) Glycosylation of CD63 impairs antibody binding, leading to more-unspecific binding in MEF cells.

lectin (Fig. 4D and E). Interestingly, standard aggregation consistently showed slightly stronger responses of the CD63-deficient platelets, which was seen as a reduced reversibility of aggregation at low or intermediate agonist concentrations (Fig. 4C). However, this had no significant effect on adhesion and thrombus formation on collagen under flow conditions (1,000 s^{-1}), which were indistinguishable between wild-type and mutant platelets (Fig. 4B). In addition, we saw no alteration of

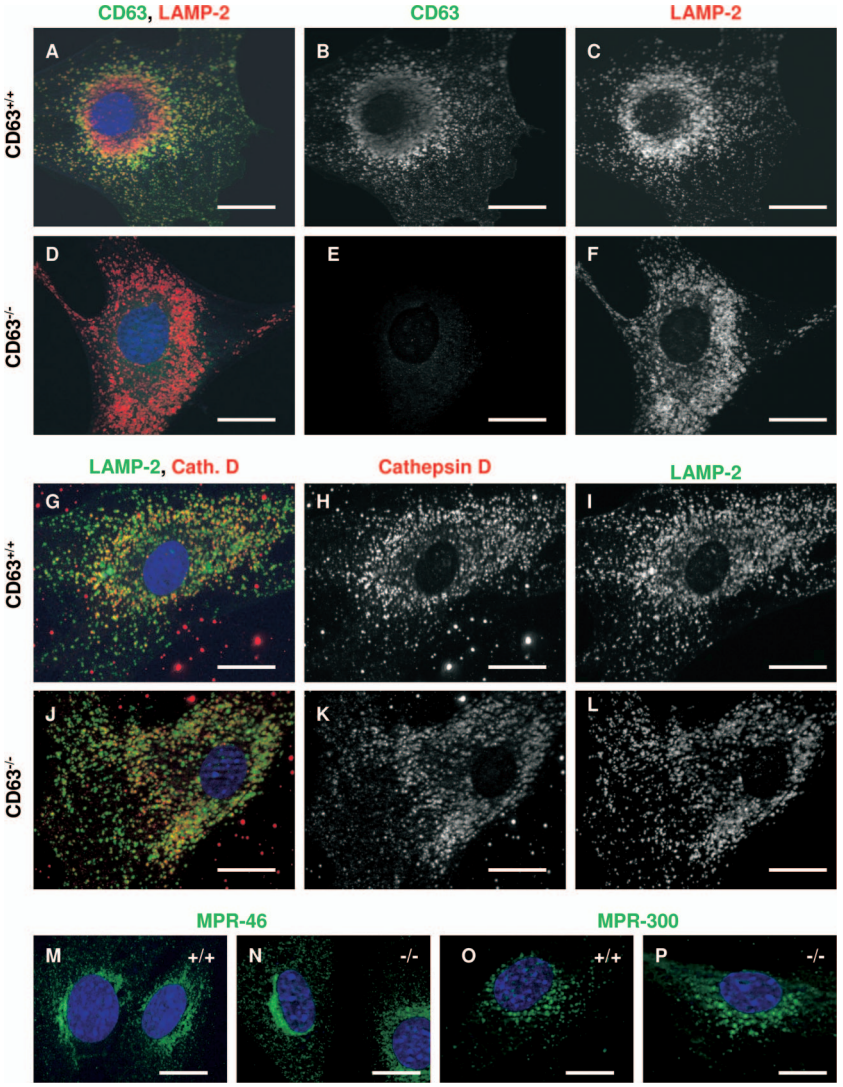

FIG. 3. Immunocytochemical analysis of CD63-deficient MEF. $CD63^{+/+}$ and $CD63^{-/-}$ MEF were fixed with 4% paraformaldehyde-PBS and immunostained against CD63 (green) and LAMP-2 (red) (A to F), cathepsin D (red) and LAMP-2 (green) (G to L), MPR-46 (M, N), and MPR-300 (O, P). CD63 was readily detected in $CD63^{+/+}$ but not in $CD63^{-/-}$ MEF with the antiserum directed against native CD63. No other differences in the amounts or intracellular distributions of the lysosomal marker proteins and mannose 6-phosphate receptors were detected. Scale bar = 10 μm. Blue indicates DAPI (4′,6-diamidino-2-phenylindole) staining of the nuclei.

$FeCl_3$-induced thrombus formation in mesenteric arterioles in vivo (66), which occurred to the same extent and with the same kinetics as those in wild-type controls (data not shown). These results indicate that CD63 does not play a crucial role for platelet production and their ability to form thrombi.

$CD63^{-/-}$ mice display inclusions in the principal cells of the collecting duct in the kidney. A detailed morphological analysis of brain, liver, spleen, and lung tissues (Fig. 5A to H) did not reveal abnormalities between CD63-deficient and wild-type mice. Northern blot analysis indicated that the expression of CD63 was strongest in the kidney (Fig. 2C and data not shown). Interestingly, we observed in CD63 knockout mice an accumulation of abnormal cytoplasmic inclusions in the principal cells of the collecting duct (Fig. 5J and K), absent in wild-type cells (Fig. 5I). Ultrastructurally, the inclusions were membrane limited and contained concentrically lamellated material (Fig. 5L).

CD63-deficient mice show remarkable water diuresis. The morphological alterations in principal cells of the collecting duct in CD63 knockout mice prompted a more detailed analysis of the kidney physiology. In comparison to wild-type animals, 1-year-old CD63 knockout mice showed a significant increase in 24-h urine production (Fig. 6A), paralleled by a respective increased in water uptake (Fig. 6B). The osmolality of $CD63^{-/-}$ urine (Fig. 6C) and the urinary concentrations of the main electrolytes, phosphate, and urea (Table 2) were reduced by half compared to the levels for wild-type urine. However, the overall 24-h excretions were not altered between genotypes (Table 2). This indicates that diuresis is due to a disturbance in water rather than in salt homeostasis. In addi-

TABLE 1. Analysis of cells of the immune system of $CD63^{-/-}$ mice[a]

Site	Cell type	Description	% of PI-low cells[b]	
			$CD63^{+/+}$	$CD63^{-/-}$
Bone marrow	BLAST cells	$CD31^{high}$ $Ly6^{-}$ C^{low}	3.8 ± 0.5	4.1 ± 1.0
	Lymphoid progenitors	$CD31^{intermediate}$ $Ly6^{-}$ C^{low}	27.2 ± 1.4	24.9 ± 3.6
	Myeloid progenitors	$CD31^{pos}$ $Ly6^{-}$ C^{pos}	5.7 ± 0.8	6.7 ± 0.6
	Erythroid progenitors	$CD31^{low}$ $Ly6^{-}$ C^{low}	5.1 ± 0.4	5.1 ± 1.1
	Immature granulocytes	$CD11b^{+}$ $Gr1^{+}$	21.0 ± 0.6	18.6 ± 1.1
	Mature granulocytes	$CD11b^{++}$ $Gr1^{++}$	41.8 ± 1.6	45.5 ± 5.0
	NK cells	$CD49b^{+}$	2.0 ± 0.2	1.9 ± 0.2
	Pro-pre-B cells	$B220^{+}$ IgM^{-}	10.7 ± 0.9	9.4 ± 1.7
	Immature B cells	$B220^{+}$ IgM^{+}	5.5 ± 0.4	4.7 ± 1.2
	Mature B cells	$B220^{++}$ IgM^{+}	2.6 ± 0.6	2.9 ± 1.0
	T cells	$CD3^{+}$	4.8 ± 0.2	5.5 ± 0.9
Spleen	T cells	$CD3^{+}$	28.3 ± 2.5	27.8 ± 1.8
	Helper T cells	$CD3^{+}$ $CD4^{+}$	16.7 ± 0.6	16.6 ± 1.0
	Cytotoxic T cells	$CD3^{+}$ $CD8^{+}$	10.1 ± 1.7	9.2 ± 1.3
	Activated helper T cells	$CD3^{+}$ $CD4^{+}$ $CD69^{+}$	6.0 ± 0.9	6.1 ± 0.7
	Activated cytotoxic T cells	$CD3^{+}$ $CD8^{+}$ $CD69^{+}$	0.7 ± 0.2	1.8 ± 1.2
	B cells	$B220^{+}$	60.5 ± 2.5	56.6 ± 2.7
	Immature B cells	$B220^{+}$ IgM^{high} IgD^{low}	6.9 ± 0.8	5.9 ± 0.8
	Mature B cells	$B220^{+}$ IgM^{low} IgD^{high}	48.3 ± 2.6	42.7 ± 4.7
	NK cells	$CD49b^{+}$ $B220^{-}$	0.9 ± 0.1	0.8 ± 0.1
Lymph node	T cells	$CD3^{+}$	43.3 ± 3.1	52.0 ± 2.0
	Helper T cells	$CD3^{+}$ $CD4^{+}$	20.9 ± 1.9	25.8 ± 1.5
	Cytotoxic T cells	$CD3^{+}$ $CD8^{+}$	16.3 ± 2.3	18.7 ± 1.8
	Activated helper T cells	$CD3^{+}$ $CD4^{+}$ $CD69^{+}$	5.9 ± 0.8	6.3 ± 1.1
	Activated cytotoxic T cells	$CD3^{+}$ $CD8^{+}$ $CD69^{+}$	2.7 ± 0.4	2.6 ± 0.5
	B cells	$B220^{+}$ IgM^{+}	21.2 ± 1.0	17.3 ± 1.6
	NK cells	$CD49b^{+}$ $B220^{-}$	1.4 ± 0.1	2.3 ± 0.8
	Macrophages	$CD11b^{+}$ $Gr1^{-}$	8.2 ± 1.0	9.2 ± 2.8

[a] Numbers of different subsets of T cells, B cells, natural killer (NK) cells, granulocytes, and respective precursors were comparable between $CD63^{+/+}$ and $CD63^{-/-}$ mice as assessed with the indicated markers by fluorescence-activated cell sorting analysis of 12-month-old littermates ($n = 6$).

[b] Mean percentages ± standard errors of the means are given for groups of six animals analyzed in two independent experiments. The total numbers of cells in the bone marrow and spleen were not significantly different between $CD63^{+/+}$ and $CD63^{-/-}$ mice (for bone marrow, $3.54 \times 10^7 \pm 0.44 \times 10^7$ for $CD63^{+/+}$ and $2.97 \times 10^7 \pm 0.44 \times 10^7$ for $CD63^{-/-}$; for spleen, $9.24 \times 10^7 \pm 0.87 \times 10^7$ for $CD63^{+/+}$ and $10.40 \times 10^7 \pm 3.13 \times 10^7$ for $CD63^{-/-}$; and for lymph node, not determined). PI, propidium iodide.

tion to the renal findings, the fecal droppings of CD63-deficient mice were apparently bigger than those of wild-type animals (Fig. 6D and F), likewise caused by a significantly higher water content (Fig. 6G) and not by an increase in dry material.

DISCUSSION

Tetraspanins modulate diverse cellular activities, such as adhesion strengthening, migration, signal transduction, and proliferation (29). Their importance is underlined by the fact that mutations in tetraspanin genes are responsible for several human diseases causing mental retardation, retinal dystrophy, deafness, and end stage hereditary nephropathy (37, 87). The analysis of tetraspanin knockout mice revealed that the phenotype of individual tetraspanin-deficient mice is usually very mild (e.g., references 23, 41, 48, 53, and 78), making it very probable that certain tetraspanins act in concert. Despite the suggested importance of CD63 for a variety of cellular mechanisms, most data concerning this protein were raised in vitro. The generation and analysis of mice lacking this tetraspanin will help in understanding the role of this protein in vivo.

Generation of CD63-null mice. The generation and subsequent characterization of CD63 knockout mice were hampered by the fact that two independent gene loci for CD63 were found in the mouse genome. Apart from the genuine CD63 locus on chromosome 10, a Cd63-related sequence (Cd63rs) was found on chromosome 18, which lacks intron sequences (25), suggesting a retroviral origin for this locus. Since such a gene duplication was not detected in the genomes of monkeys and rats, it appears to have evolved relatively late in evolution (33). The lack of detectable promoter activity and the mutation in the critical tyrosine-containing motif for adapter protein 3-dependent lysosomal targeting strongly suggest that Cd63rs is both transcriptionally and functionally inactive. Deglycosylation of protein extracts derived from different cell types allowed the immunoblot detection of the CD63 polypeptide and confirmed the complete absence of CD63 expression in homozygote-deficient mouse tissues. CD63 knockout mice are fertile and viable without presenting an overt phenotype. This is somehow surprising with respect to the ubiquitous expression of CD63 (72) and its postulated major functions in different processes, such as β1 integrin-mediated cell adhesion, signal transduction in T cells and mast cells, and translocation of the H^+ K^+ ATPase in the colon and stomach (12, 16, 45, 62). The mild phenotype of the $CD63^{-/-}$ mice is in contrast to previously characterized mice with deficiencies in other major lysosomal membrane proteins, such as LAMP-2 (77) and LIMP-2 (22). These mice often die early after birth and show

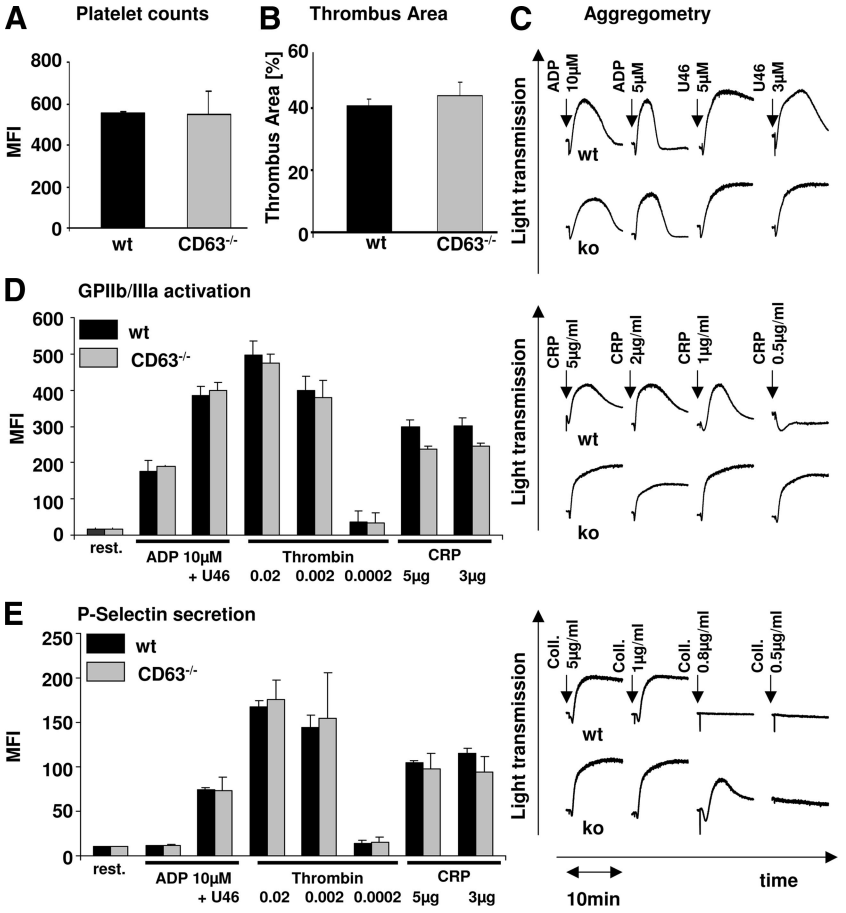

FIG. 4. Analysis of $CD63^{-/-}$ platelets. (A) CD63-deficient mice possess normal platelet numbers ($n = 9$). MFI, mean fluorescence intensity; wt, wild type. (B) CD63 is not essential for platelet adhesion to collagen under flow. Whole-blood samples from the indicated mice ($n = 15$) were perfused at wall shear rates of 1,000 s^{-1} (4 min) over a collagen-coated surface. The thrombus area, meaning the area covered with platelets, was determined for phase-contrast images. Similar results have been obtained under low shear rates of 150 s^{-1} (10 min). (C) Heparinized platelet-rich plasma samples from wild-type and CD63-deficient (ko) mice were stimulated with the indicated concentrations of ADP, U46619, CRP, or collagen (coll.), and light transmission was recorded with a standard aggregometer. Representative results for each genotype are shown ($n = 3$). CD63-deficient platelets seem to respond more strongly to collagen or CRP. (D, E) Diluted whole-blood samples were stimulated with ADP (10 μM) ± U46619 (U46; 1 μM), thrombin (0.02 U/ml, 0.002 U/ml, or 0.0002 U/ml), or CRP (5 μg/ml or 3 μg/ml) for 2 min each; subsequently incubated with anti-activated GPIIbIIIa (D) or anti-P-selectin (E) for 10 min; and analyzed directly. Platelets were gated by forward-scatter/side-scatter characteristics. No changes in activation were detected between wild-type and CD63-deficient platelets. rest., resting/unstimulated.

multiple tissue pathologies. The common tissue expression of the three tetraspanins CD63, CD9, and CD151 (72) suggests that they also share some functions and that the individual deficiency of one of these proteins may be well compensated for by the other proteins.

Lysosomes are not affected when CD63 is missing. At steady state, CD63 is mainly localized within the lysosomal membrane (Fig. 1B and 3A to F). However, the lack of CD63 affected neither the morphology or distribution of lysosomes nor their functions, such as acidification, endocytosis, autophagy, and the activities and expression of lysosomal hydrolases. The lack of a lysosome-related phenotype suggests that the steady-state localization of CD63 does not necessarily correlate with the place where CD63 is needed. Indeed, CD63 can be translocated to the plasma membrane, where it may be involved in adhesion of granulocytes to endothelial cells (79).

Normal hematopoiesis and platelet function in CD63-null mice. Due to the relatively high expression of CD63 in immune cells, such as macrophages and neutrophil granulocytes, and since a number of tetraspanin knockout mice displayed B- and T-cell abnormalities (41, 48, 53, 78, 80, 81, 84), the numbers of different populations of immune cells in the knockout mice were systematically analyzed (Table 1). No differences between the genotypes were noted, suggesting also here an efficient compensation of CD63 deficiency, most likely through other tetraspanins, like CD9. CD63 may be involved in the integrin-dependent endocytosis and migration capacities of immature dendritic cells (52, 83) but also be able to modulate major histocompatibility complex class II transport to the cell surface (83). Preliminary experiments using labeled ovalbumin did not reveal differences in antigen processing in wild-type and CD63 knockout macrophages and dendritic cells (data not shown).

One of the major functions for CD63 was postulated in the regulation of platelet activity (35). Antibody inhibition of CD63 did not affect the adhesion of platelets on fibrinogen, collagen, laminin, or fibronectin but resulted in an impaired

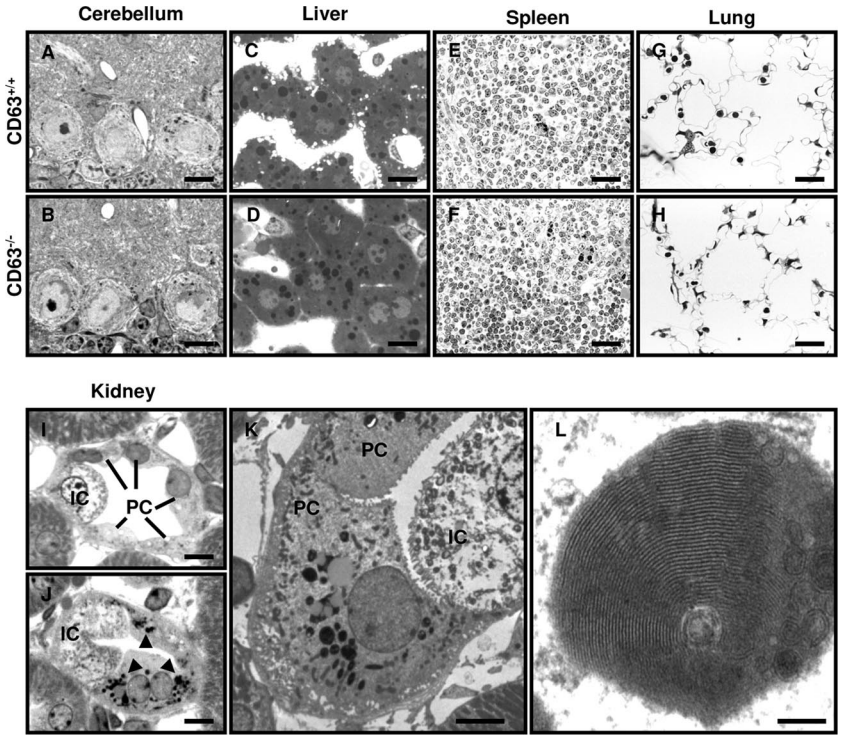

FIG. 5. Histology of $CD63^{-/-}$ mice. (A to J) One-micrometer-thick semithin sections, stained with Toluidin blue. In cerebellar Purkinje cells (A, B), the liver (C, D), splenic white pulp (E, F), and the lung (G, H), no morphological differences between $CD63^{+/+}$ (upper row) and $CD63^{-/-}$ (lower row) mice can be seen. The dense inclusions seen in hepatocytes correspond to lipid droplets. (I, J) Kidney, outer medullary collecting ducts. PC, principal cells; IC, intercalated cells. In the $CD63^{-/-}$ mouse (J), the PCs (arrowheads) show dense cytoplasmic inclusions, which are absent from PC in the $CD63^{+/+}$ mouse (I). (K) Low electron-microscopic magnification showing PCs of a $CD63^{-/-}$ mouse with abnormal inclusions. (L) At high resolution, the abnormal inclusions show a concentrically lamellar pattern. Scale bars = 10 μm (A to D), 25 μm (E to H), 10 μm (I and J), 3 μm (K), and 0.1 μm (L).

spreading of platelets on a fibronectin-coated surface (35, 36). In contrast, our in vitro and in vivo studies did not reveal major abnormalities in CD63-deficient platelets, although a reduced reversibility of aggregation that we cannot explain at present was consistently observed. Possibly, CD63 acts as a negative regulator of sustained signaling or prolonged integrin activation in these cells, but this effect is of limited importance under conditions of flow ex vivo (Fig. 4B) or in the well-established model of $FeCl_3$-induced thrombus formation in vivo (not shown) (66). The candidates for proteins which may compensate for the loss of CD63 are the tetraspanins CD9 (36), TSSC6, and CD151 (24, 84). These proteins have also been shown to interact with αIIbβ3 integrin dimers at the cell surfaces of platelets.

Kidney pathology and disturbed water balance in CD63-null mice. Despite the fact that most of what is known about CD63 function is based on the hematopoietic system, the strongest expression of CD63 was found in the kidney (data not shown) (72). An obvious morphological abnormality seen in CD63 knockout mice was the accumulation of lamellar inclusions in the principal cells of the collecting duct. Metabolic analysis of these mice revealed that CD63 knockout mice displayed an altered water balance, with a significantly increased water loss via the kidney as well as via the gastrointestinal tract. For water homeostasis, the kidney is the most relevant organ and is acutely regulated by vasopressin (70). Vasopressin controls the trafficking of the water channel aquaporin-2 (AQP-2) to the luminal plasma membrane (71). Therefore, alterations in the intracellular distribution of AQP-2 due to the lack of CD63 might be considered a reason for the overt water diuresis. First experiments indicate that in the collecting duct of CD63 knockout mice, AQP-2 was still transported to the apical membrane (data not shown). However, a partial reduction of AQP-2 trafficking to the membrane could be responsible for the polyuria and polydipsia observed in CD63 knockout mice.

Lamellar inclusion bodies similar to the ones observed in our mice have been reported in the context of trafficking abnormalities. Rab proteins are small GTPases involved in vesicle cycling. In the kidney inner medullary collecting duct, for example, they are associated with AQP2-containing intracellular vesicles (4). Mice with mutations in Rab38 show an abnormal lung phenotype, with a pronounced accumulation of lamellar bodies of increased size and number, in alveolar epithelial cells (60). In these lamellar bodies, phosphatidylcholine and phospholipids were enriched. Cytoplasmic inclusions as observed in CD63 knockout mice, hence, could represent vesicular accumulation of membrane stacks.

With respect to CD63 and transport protein regulation, it has been reported that overexpression of CD63 in Cos7 cells led to an increased endocytosis of the gastric-type H^+ K^+ ATPase (16), and knockdown of CD63 resulted in a higher degree of surface expression of the colon type H^+ K^+ ATPase

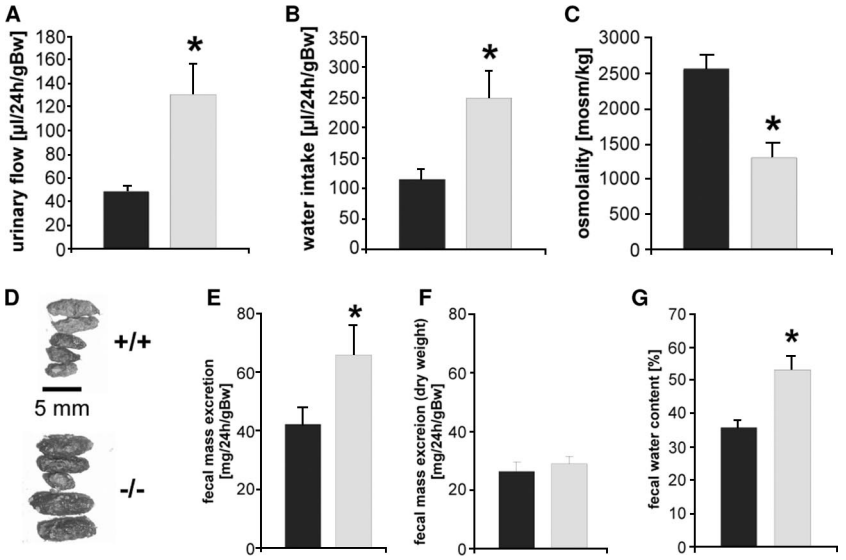

FIG. 6. Metabolic analysis of CD63-deficient mice. Eight 11- to 12-month-old female mice (black, $CD63^{+/+}$; gray, $CD63^{-/-}$) in metabolic cages were analyzed for 24 h. (A) $CD63^{-/-}$ mice urinate three times more within 24 h and per gram of body weight (Bw). (B) CD63-deficient mice drink significantly more as well. (C) The osmolality of CD63 urine is significantly reduced. (D) Fecal droppings of CD63-deficient mice are bigger than those of wild-type animals. (E) The total amount of feces per gram body weight is significantly increased as well. (F, G) The increased fecal secretion is due not to increased dry weight but to a significantly higher water content.

(13). It is therefore conceivable that the functions of other membrane proteins involved in epithelial electrolyte and water transport might be affected by CD63 deficiency. As a candidate, the potassium channel ROMK1 (renal outer medullary potassium channel), located in the luminal membranes of principal cells of the collecting duct, has to be considered. It was recently shown that CD63 in concert with the receptor-bound protein tyrosine phosphatase a (RPTPa), a type 1 transmembrane protein (15), leads to an activation of c-Src and a subsequent endocytosis and inactivation of ROMK1 (47).

Another tetraspanin, CD151, is associated with kidney function (37, 68). CD151-deficient mice, as well as patients with nonsense mutations in CD151, display renal failure and massive proteinuria, with severe alterations of podocytes and glomerulosclerosis. Therefore, CD151 is the main tetraspanin associated with the laminin-binding integrins α3/β1, α6/β1, and α7/β1, essential for anchorage of cells in the extracellular matrix (11, 29, 74, 75). Unlike the situation seen in CD151 knockout mice (68), no glomerular or comparable tubular abnormalities and no proteinuria were observed in CD63 knockout mice (data not shown), suggesting that these two tetraspanins are responsible for different functions in the kidney and are not able to compensate for each other.

TABLE 2. Urinary concentrations and total urinary excretions of different substances within 24 h[a]

Mouse type and substance	Urine concn (mmol/liter)	Total excretion (μmol/24 h/g body weight)
$CD63^{+/+}$		
Na^+	168.13 ± 6.40	8.03 ± 0.80
K^+	423.54 ± 7.84	18.16 ± 3.34
Cl^-	216.88 ± 11.3	10.49 ± 1.25
Ca^{2+}	3.29 ± 0.46	0.15 ± 0.02
Phosphate	27.33 ± 5.51	1.25 ± 0.24
Urea	1587 ± 59	74.79 ± 7.35
Creatinine	3.26 ± 0.30	
$CD63^{-/-}$		
Na^+	89.38 ± 8.63*	10.39 ± 1.53
K^+	199.71 ± 34.96*	20.63 ± 1.53
Cl^-	107.50 ± 12.61*	12.18 ± 1.65
Ca^{2+}	1.70 ± 0.39*	0.16 ± 0.03
Phosphate	18.96 ± 4.94*	1.54 ± 0.38
Urea	719 ± 123*	74.13 ± 6.83
Creatinine	1.21 ± 0.33*	

[a] $n = 8$. *, $P < 0.05$.

Conclusions. Despite the ubiquitous expression of CD63 and the many postulated functions of this tetraspanin, the phenotype of mice lacking CD63 is a relatively mild one. This supports the idea that, like other proteins of the tetraspanin superfamily, CD63 needs partners to accomplish specific functions. It may well be that under certain challenge conditions or in specific pathological situations, the hidden roles of CD63 are uncovered. CD63-deficient mice will be very helpful in addressing these specific questions.

ACKNOWLEDGMENTS

We thank Dagmar Niemeier, Sebastian Held, Katrin Westphal, Thomas Stegmann, Marlies Rusch, and Katharina Stiebeling for their excellent technical assistance, Mirka Pozgajova for help in performing the platelet analysis, and Friedrich Haag for antibody supply.

J.S. was supported through the Böhringer Ingelheim Fonds (BIF). P.S. was supported through the Deutsche Forschungsgemeinschaft, SA683/5-1, and the Inflammation at Interfaces Cluster of Excellence.

REFERENCES

1. **Atkinson, B., C. S. Ernst, B. F. D. Ghrist, M. Herlyn, M. Blaszczyk, A. H. Ross, D. Herlyn, Z. Steplewski, and H. Koprowski.** 1984. Identification of melanoma-associated antigens using fixed tissue screening of antibodies. Cancer Res. **44:**2577–2581.

2. **Atkinson, B., C. S. Ernst, B. F. D. Ghrist, A. H. Ross, W. H. Clark, M. Herlyn, D. Herlyn, G. Maul, Z. Steplewski, and H. Koprowski.** 1985. Monoclonal antibody to a highly glycosylated protein reacts in fixed tissue with melanoma and other tumors. Hybridoma **4:**243–255.
3. **Azorsa, D. O., J. A. Hyman, and J. E. K. Hildreth.** 1991. Cd63/Pltgp40: a platelet activation antigen identical to the stage-specific, melanoma-associated antigen Me491. Blood **78:**280–284.
4. **Barile, M., T. Pisitkun, M. J. Yu, C. L. Chou, M. J. Verbalis, R. F. Shen, and M. A. Knepper.** 2005. Large scale protein identification in intracellular aquaporin-2 vesicles from renal inner medullary collecting duct. Mol. Cell. Proteomics **4:**1095–1106.
5. **Beinert, T., S. Munzing, K. Possinger, and F. Krombach.** 2000. Increased expression of the tetraspanins CD53 and CD63 on apoptotic human neutrophils. J. Leukoc. Biol. **67:**369–373.
6. **Berditchevski, F., G. Bazzoni, and M. E. Hemler.** 1995. Specific association of Cd63 with the Vla-3 and Vla-6 integrins. J. Biol. Chem. **270:**17784–17790.
7. **Berditchevski, F., and E. Odintsova.** 2007. Tetraspanins as regulators of protein trafficking. Traffic **8:**89–96.
8. **Berditchevski, F., K. F. Tolias, K. Wong, C. L. Carpenter, and M. E. Hemler.** 1997. A novel link between integrins, transmembrane-4 superfamily proteins (CD63 and CD81), and phosphatidylinositol 4-kinase. J. Biol. Chem. **272:** 2595–2598.
9. **Berditchevski, F., M. M. Zutter, and M. E. Hemler.** 1996. Characterization of novel complexes on the cell surface between integrins and proteins with 4 transmembrane domains (TM4 proteins). Mol. Biol. Cell **7:**193–207.
10. **Bergmeier, W., V. Schulte, G. Brockhoff, U. Bier, H. Zirngibl, and B. Nieswandt.** 2002. Flow cytometric detection of activated mouse integrin αIIbβ3 with a novel monoclonal antibody. Cytometry **48:**80–86.
11. **Boucheix, C., and E. Rubinstein.** 2001. Tetraspanins. Cell. Mol. Life Sci. **58:**1189–1205.
12. **Claussen, M., D. Buergisser, A. G. P. Schuller, U. Matzner, and T. Braulke.** 1995. Regulation of insulin-like growth factor (Igf)-binding protein-6 and mannose 6-phosphate/IGF-II receptor expression in IGF-IL-overexpressing NIH 3T3 cells. Mol. Endocrinol. **9:**902–912.
13. **Codina, J., J. Li, and T. D. Dubose.** 2005. CD63 interacts with the carboxy terminus of the colonic H+-K+-ATPase to increase plasma membrane localization and 86Rb(+) uptake. Am. J. Physiol. Cell Physiol. **288:**C1279–C1286.
14. **de Bruijn, M. F. T. R., W. Van Vianen, R. E. Ploemacher, I. A. J. M. Bakker-Woudenberg, P. A. Campbell, W. van Ewijk, and P. J. M. Leenen.** 1998. Bone marrow cellular composition in Listeria monocytogenes infected mice detected using ER-MP12 and ER-MP20 antibodies: a flow cytometric alternative to differential counting. J. Immunol. Methods **217:**27–39.
15. **den Hertog, J., C. Blanchetot, A. Buist, J. Overvoorde, A. Van der Sar, and L. G. J. Tertoolen.** 1999. Receptor protein-tyrosine phosphatase signalling in development. Int. J. Dev. Biol. **43:**723–733.
16. **Duffield, A. S., E. Kamsteeg, A. N. Brown, and M. J. Caplan.** 2003. Association with the tetraspanin CD63 enhances the internalization of the H,K-ATPase beta-subunit. Mol. Biol. Cell **13:**516A.
17. **Engering, A., L. Kuhn, D. Fluitsma, E. Hoefsmit, and J. Pieters.** 2003. Differential post-translational modification of CD63 molecules during maturation of human dendritic cells. Eur. J. Biochem. **270:**2412–2420.
18. **Engering, A., and J. Pieters.** 2001. Association of distinct tetraspanins with MHC class II molecules at different subcellular locations in human immature dendritic cells. Int. Immunol. **13:**127–134.
19. **Ernst, C. S., J. W. Shen, S. Litwin, M. Herlyn, H. Koprowski, and H. F. Sears.** 1986. Multiparameter evaluation of the expression in situ of normal and tumor-associated antigens in human colorectal-carcinoma. J. Natl. Cancer Inst. **77:**387–395.
20. **Escribano, L., A. Orfao, B. D. Agustin, C. Cervero, S. Herrero, J. Villarrubia, P. Bravo, A. Torrelo, T. Montero, M. Valdemoro, J. L. Velasco, J. L. Navarro, and J. F. San Miguel.** 1998. Human bone marrow mast cells from indolent systemic mast cell disease constitutively express increased amounts of the CD63 protein on their surface. Cytometry **34:**223–228.
21. **Fukuda, M.** 1991. Lysosomal membrane glycoproteins. Structure, biosynthesis, and intracellular trafficking. J. Biol. Chem. **266:**21327–21330.
22. **Gamp, A. C., Y. Tanaka, R. Lüllmann-Rauch, D. Wittke, R. D'Hooge, P. P. De Deyn, T. Moser, H. Maier, D. Hartmann, K. Reiss, A. L. Illert, K. von Figura, and P. Saftig.** 2003. LIMP-2/LGP85 deficiency causes ureteric pelvic junction obstruction, deafness and peripheral neuropathy in mice. Hum. Mol. Genet. **12:**631–646.
23. **Geisert, E. E., R. W. Williams, G. R. Geisert, L. Fan, A. M. Asbury, H. T. Maecker, J. Deng, and S. Levy.** 2002. Increased brain size and glial cell number in CD81-null mice. J. Comp. Neurol. **453:**22–32.
24. **Goschnick, M. W., L. M. Lau, J. L. Wee, Y. S. Liu, P. M. Hogarth, L. M. Robb, M. J. Hickey, M. D. Wright, and D. E. Jackson.** 2006. Impaired "outside-in" integrin alpha(IIb)beta(3) signaling and thrombus stability in TSSC6-deficient mice. Blood **108:**1911–1918.
25. **Gwynn, B., E. M. Eicher, and L. L. Peters.** 1996. Genetic localization of Cd63, a member of the transmembrane 4 superfamily, reveals two distinct loci in the mouse genome. Genomics **35:**389–391.
26. **Hammond, C., L. K. Denzin, M. Pan, J. M. Griffith, H. J. Geuze, and P. Cresswell.** 1998. The tetraspan protein CD82 is a resident of MHC class II compartments where it associates with HLA-DR, -DM, and -DO molecules. J. Immunol. **161:**3282–3291.
27. **Heijnen, H. F. G., N. Debili, W. Vainchencker, J. Breton-Gorius, H. J. Geuze, and J. J. Sixma.** 1998. Multivesicular bodies are an intermediate stage in the formation of platelet alpha-granules. Blood **91:**2313–2325.
28. **Hemler, M. E.** 2001. Specific tetraspanin functions. J. Cell Biol. **155:**1103–1107.
29. **Hemler, M. E.** 2005. Tetraspanin functions and associated microdomains. Nat. Rev. Mol. Cell Biol. **6:**801–811.
30. **Hildreth, J. E. K., D. Derr, and D. O. Azorsa.** 1991. Characterization of a novel self-associating Mr 40,000 platelet glycoprotein. Blood **77:**121–132.
31. **Hogan, B., F. Constantini, and E. Lacy.** 1986. Manipulating the mouse: a laboratory manual. Cold Spring Harbor Laboratory, Cold Spring Harbor, NY.
32. **Hooper, M., K. Hardy, A. Handyside, S. Hunter, and M. Monk.** 1987. HPRT-deficient (Lesch-Nyhan) mouse embryos derived from germline colonization by cultured cells. Nature **326:**292–295.
33. **Hotta, H., A. H. Ross, K. Huebner, M. Isobe, S. Wendeborn, M. V. Chao, R. P. Ricciardi, Y. Tsujimoto, C. M. Croce, and H. Koprowski.** 1988. Molecular cloning and characterization of an antigen associated with early stages of melanoma tumor progression. Cancer Res. **48:**2955–2962.
34. **Israels, S. J., J. M. Gerrard, Y. V. Jacques, A. Mcnicol, B. Cham, M. Nishibori, and D. F. Bainton.** 1992. Platelet dense granule membranes contain both granulophysin and P-selectin (Gmp-140). Blood **80:**143–152.
35. **Israels, S. J., and E. M. McMillan-Ward.** 2005. CD63 modulates spreading and tyrosine phosphorylation of platelets on immobilized fibrinogen. Thromb. Haemost. **93:**311–318.
36. **Israels, S. J., E. M. McMillan-Ward, J. Easton, C. Robertson, and A. Mcnicol.** 2001. CD63 associates with the alpha(IIb)beta(3) integrin-CD9 complex on the surface of activated platelets. Thromb. Haemost. **85:**134–141.
37. **Karamatic Crew, V., N. Burton, A. Kagan, C. A. Green, C. Levene, F. Flinter, R. L. Brady, G. Daniels, and D. J. Anstee.** 2004. CD 151, the first member of the tetraspanin (TM4) superfamily detected on erythrocytes, is essential for the correct assembly of human basement membranes in kidney and skin. Blood **104:**2217–2223.
38. **Kitani, S., E. Berenstein, S. Mergenhagen, P. Tempst, and R. P. Siraganian.** 1991. A cell surface glycoprotein of rat basophilic leukemia cells close to the high affinity Ige receptor (Fc epsilon Ri). Similarity to human melanoma differentiation antigen Me491. J. Biol. Chem. **266:**1903–1909.
39. **Kleine-Tebbe, J., S. Erdmann, E. F. Knol, D. W. MacGlashan, L. K. Poulsen, and B. F. Gibbs.** 2006. Diagnostic tests based on human basophils: potentials, pitfalls and perspectives. Int. Arch. Allergy Immunol. **141:**79–90.
40. **Klumperman, J., A. Hille, T. Veenendaal, V. Oorschot, W. Stoorvogel, K. von Figura, and H. J. Geuze.** 1993. Differences in the endosomal distributions of the 2 mannose 6-phosphate receptors. J. Cell Biol. **121:**997–1010.
41. **Knobeloch, K. P., M. D. Wright, A. F. Ochsenbein, O. Liesenfeld, J. Lohler, R. M. Zinkernagel, I. Horak, and Z. Orinska.** 2000. Targeted inactivation of the tetraspanin CD37 impairs T-cell-dependent B-cell response under suboptimal costimulatory conditions. Mol. Cell. Biol. **20:**5363–5369.
42. **Kobayashi, T., U. M. Vischer, C. Rosnoblet, C. Lebrand, M. Lindsay, R. G. Parton, E. K. O. Kruithof, and J. Gruenberg.** 2000. The tetraspanin CD63/lamp3 cycles between endocytic and secretory compartments in human endothelial cells. Mol. Biol. Cell **11:**1829–1843.
43. **Koch-Nolte, F., G. Glowacki, P. Bannas, F. Braasch, G. Dubberke, E. Ortolan, A. Funaro, F. Malavasi, and F. Haag.** 2005. Use of genetic immunization to raise antibodies recognizing toxin-related cell surface ADP-ribosyltransferases in native conformation. Cell. Immunol. **236:**66–71.
44. **Koyama, Y., B. Yamanoha, and T. Yoshida.** 1990. A Novel monoclonal antibody induces the differentiation of monocyte leukemic cells. Biochem. Biophys. Res. Commun. **168:**898–904.
45. **Kraft, S., T. Fleming, J. M. Billingsley, S. Y. Lin, M. H. Jouvin, P. Storz, and J. P. Kinet.** 2005. Anti-CD63 antibodies suppress IgE-dependent allergic reactions in vitro and in vivo. J. Exp. Med. **201:**385–396.
46. **Levy, S., and T. Shoham.** 2005. Protein-protein interactions in the tetraspanin web. Physiology **20:**218–224.
47. **Lin, D. H., E. J. Kamsteeg, Y. Zhang, Y. Jin, H. Sterling, P. Yue, M. Roos, A. Duffield, J. Spencer, M. Caplan, and W. H. Wang.** 2008. Expression of tetraspan protein CD63 activates protein-tyrosine kinase (PTK) and enhances the PTK-induced inhibition of ROMK channels. J. Biol. Chem. **283:**7674–7681.
48. **Maecker, H. T., and S. Levy.** 1997. Normal lymphocyte development but delayed humoral immune response in CD81-null mice. J. Exp. Med. **185:** 1505–1510.
49. **Maecker, H. T., S. C. Todd, and S. Levy.** 1997. The tetraspanin superfamily: molecular facilitators. FASEB J. **11:**428–442.
50. **Mahmudi-Azer, S., G. P. Downey, and R. Moqbel.** 2002. Translocation of the tetraspanin CD63 in association with human eosinophil mediator release. Blood **99:**4039–4047.
51. **Mannion, B. A., F. Berditchevski, S. K. Kraeft, L. B. Chen, and M. E. Hemler.** 1996. Transmembrane-4 superfamily proteins CD81 (TAPA-1), CD82, CD63, and CD53 specifically associate with integrin alpha(4)beta(1) (CD49d/CD29). J. Immunol. **157:**2039–2047.

52. **Mantegazza, A. R., M. M. Barrio, S. Moutel, L. Bover, M. Weck, P. Brossart, J. L. Teillaud, and J. Mordoh.** 2004. CD63 tetraspanin slows down cell migration and translocates to the endosomal-lysosomal-MIICs route after extracellular stimuli in human immature dendritic cells. Blood **104:**1183–1190.
53. **Miyazaki, T., U. Muller, and K. S. Campbell.** 1997. Normal development but differentially altered proliferative responses of lymphocytes in mice lacking CD81. EMBO J. **16:**4217–4225.
54. **Nieswandt, B., W. Bergmeier, K. Rackebrandt, J. E. Gessner, and H. Zirngibl.** 2000. Identification of critical antigen-specific mechanisms in the development of immune thrombocytopenic purpura in mice. Blood **96:**2520–2527.
55. **Nieswandt, B., W. Bergmeier, V. Schulte, K. Rackebrandt, J. E. Gessner, and H. Zirngibl.** 2000. Expression and function of the mouse collagen receptor glycoprotein VI is strictly dependent on its association with the FcR gamma chain. J. Biol. Chem. **275:**23998–24002.
56. **Nieswandt, B., C. Brakebusch, W. Bergmeier, V. Schulte, D. Bouvard, R. Mokhtari-Nejad, T. Lindhout, J. W. M. Heemskerk, H. Zirngibl, and R. Fassler.** 2001. Glycoprotein VI but not alpha 2 beta 1 integrin is essential for platelet interaction with collagen. EMBO J. **20:**2120–2130.
57. **Nieswandt, B., V. Schulte, W. Bergmeier, R. Mokhtari-Nejad, K. Rackebrandt, J. P. Cazenave, P. Ohlmann, C. Gachet, and H. Zirngibl.** 2001. Long-term antithrombotic protection by in vivo depletion of platelet glycoprotein VI in mice. J. Exp. Med. **193:**459–469.
58. **Nishibori, M., B. Cham, A. Mcnicol, A. Shalev, N. Jain, and J. M. Gerrard.** 1993. The protein Cd63 is in platelet dense granules, is deficient in a patient with Hermansky-Pudlak syndrome, and appears identical to granulophysin. J. Clin. Investig. **91:**1775–1782.
59. **Nishikata, H., C. Oliver, S. E. Mergenhagen, and R. P. Siraganian.** 1992. The rat mast cell antigen AD1 (homolog to human CD63 or melanoma antigen ME491) is expressed in other cells in culture. J. Immunol. **149:**862–870.
60. **Osanai, K., R. Oikawa, J. Higuchi, M. Kobayashi, K. Tsuchihara, M. Iguchi, H. Jongsu, H. Toga, and D. R. Voelker.** 2008. A mutation in Rab38 small GTPase causes abnormal lung surfactant homeostasis and aberrant alveolar structure in mice. Am. J. Pathol. **173:**1265–1274.
61. **Peters, P. J., J. Borst, V. Oorschot, M. Fukuda, O. Krahenbuhl, J. Tschopp, J. W. Slot, and H. J. Geuze.** 1991. Cytotoxic lymphocyte-T granules are secretory lysosomes, containing both perforin and granzymes. J. Exp. Med. **173:**1099–1109.
62. **Pfistershammer, K., O. Majdic, J. Stockl, G. Zlabinger, S. Kirchberger, P. Steinberger, and W. Knapp.** 2004. CD63 as an activation-linked T cell costimulatory element. J. Immunol. **173:**6000–6008.
63. **Pohlmann, R., M. W. C. Boeker, and K. von Figura.** 1995. The 2 mannose 6-phosphate receptors transport distinct complements of lysosomal proteins. J. Biol. Chem. **270:**27311–27318.
64. **Polasek, J.** 2004. Procoagulant potential of platelet alpha granules. Platelets **15:**403–407.
65. **Radford, K. J., R. F. Thorne, and P. Hersey.** 1996. CD63 associates with transmembrane 4 superfamily members, CD9 and CD81, and with beta 1 integrins in human melanoma. Biochem. Biophys. Res. Commun. **222:**13–18.
66. **Renne, T., M. Pozgajova, S. Gruner, K. Schuh, H. U. Pauer, P. Burfeind, D. Gailani, and B. Nieswandt.** 2005. Defective thrombus formation in mice lacking coagulation factor XII. J. Exp. Med. **202:**271–281.
67. **Rous, B. A., B. J. Reaves, G. Ihrke, J. A. G. Briggs, S. R. Gray, D. J. Stephens, G. Banting, and J. P. Luzio.** 2002. Role of adaptor complex AP-3 in targeting wild-type and mutated CD63 to lysosomes. Mol. Biol. Cell **13:**1071–1082.
68. **Sachs, N., M. Kreft, M. A. V. Weerman, A. J. Beynon, T. A. Peters, J. J. Weening, and A. Sonnenberg.** 2006. Kidney failure in mice lacking the tetraspanin CD151. J. Cell Biol. **175:**33–39.
69. **Saftig, P., C. Peters, K. von Figura, K. Craessaerts, F. VanLeuven, and B. DeStrooper.** 1996. Amyloidogenic processing of human amyloid precursor protein in hippocampal neurons devoid of cathepsin D. J. Biol. Chem. **271:**27241–27244.
70. **Samarasinghe, S., and T. Vokes.** 2006. Diabetes insipidus. Expert Rev. Anticancer Ther. **6:**S63–S74.
71. **Sasaki, S., and Y. Noda.** 2007. Aquaporin-2 protein dynamics within the cell. Curr. Opin. Nephrol. Hypertens. **16:**348–352.
72. **Sincock, P. M., G. Mayrhofer, and L. K. Ashman.** 1997. Localization of the transmembrane 4 superfamily (TM4SF) member PETA-3 (CD151) in normal human tissues: comparison with CD9, CD63, and alpha 5 beta 1 integrin. J. Histochem. Cytochem. **45:**515–525.
73. **Smith, M., R. Bleijs, K. Radford, and P. Hersey.** 1997. Immunogenicity of CD63 in a patient with melanoma. Melanoma Res. **7:**S163–S170.
74. **Sterk, L. M. T., C. A. W. Geuijen, L. C. J. M. Oomen, J. Calafat, H. Janssen, and A. Sonnenberg.** 2000. The tetraspan molecule CD151, a novel constituent of hemidesmosomes, associates with the integrin alpha 6 beta 4 and may regulate the spatial organization of hemidesmosomes. J. Cell Biol. **149:**969–982.
75. **Sterk, L. M. T., C. A. W. Geuijen, J. G. van den Berg, N. Claessen, J. J. Weening, and A. Sonnenberg.** 2002. Association of the tetraspanin CD151 with the laminin-binding integrins alpha 3 beta 1, alpha 6 beta 1, alpha 6 beta 4 and alpha 7 beta 1 in cells in culture and in vivo. J. Cell Sci. **115:**1161–1173.
76. **Stipp, C. S., T. V. Kolesnikova, and M. E. Hemler.** 2003. Functional domains in tetraspanin proteins. Trends Biochem. Sci. **28:**106–112.
77. **Tanaka, Y., G. Guhde, A. Suter, E. L. Eskelinen, D. Hartmann, R. Lüllmann-Rauch, P. M. L. Janssen, J. Blanz, K. von Figura, and P. Saftig.** 2000. Accumulation of autophagic vacuoles and cardiomyopathy in LAMP-2-deficient mice. Nature **406:**902–906.
78. **Tarrant, J. A., J. Groom, D. Metcalf, R. L. Li, B. Borobokas, M. D. Wright, D. Tarlinton, and L. Robb.** 2002. The absence of *Tssc6*, a member of the tetraspanin superfamily, does not affect lymphoid development but enhances in vitro T-cell proliferative responses. Mol. Cell. Biol. **22:**5006–5018.
79. **Toothill, V. J., J. A. Vanmourik, H. K. Niewenhuis, M. J. Metzelaar, and J. D. Pearson.** 1990. Characterization of the enhanced adhesion of neutrophil leukocytes to thrombin-stimulated endothelial cells. J. Immunol. **145:**283–291.
80. **Tsitsikov, E. N., J. C. Gutierrez-Ramos, and R. S. Geha.** 1997. Impaired CD19 expression and signaling, enhanced antibody response to type II T independent antigen and reduction of B-1 cells in CD81-deficient mice. Proc. Natl. Acad. Sci. USA **94:**10844–10849.
81. **van Spriel, A. B., K. L. Puls, M. Sofi, D. Pouniotis, H. Hochrein, Z. Orinska, K. P. Knobeloch, M. Plebanski, and M. D. Wright.** 2004. A regulatory role for CD37 in T cell proliferation. J. Immunol. **172:**2953–2961.
82. **von Lindern, J. J., D. Rojo, K. Grovit-Ferbas, C. Yeramian, C. Deng, G. Herbein, M. R. Ferguson, T. C. Pappas, J. M. Decker, A. Singh, R. G. Collman, and W. A. O'Brien.** 2003. Potential role for CD63 in CCR5-mediated human immunodeficiency virus type 1 infection of macrophages. J. Virol. **77:**3624–3633.
83. **Vyas, J. M., Y. M. Kim, K. Artavanis-Tsakonas, J. C. Love, A. G. Van der Veen, and H. L. Ploegh.** 2007. Tubulation of class II MHC compartments is microtubule dependent and involves multiple endolysosomal membrane proteins in primary dendritic cells. J. Immunol. **178:**7199–7210.
84. **Wright, M. D., S. M. Geary, S. Fitter, G. W. Moseley, L. M. Lau, K. C. Sheng, V. Apostolopoulos, E. G. Stanley, D. E. Jackson, and L. K. Ashman.** 2004. Characterization of mice lacking the tetraspanin superfamily member CD151. Mol. Cell. Biol. **24:**5978–5988.
85. **Yauch, R. L., and M. E. Hemler.** 2000. Specific interactions among transmembrane 4 superfamily (TM4SF) proteins and phosphoinositide 4-kinase. Biochem. J. **351:**629–637.
86. **Yunta, M., and P. A. Lazo.** 2003. Tetraspanin proteins as organisers of membrane microdomains and signalling complexes. Cell. Signal. **15:**559–564.
87. **Zemni, R., T. Bienvenu, M. C. Vinet, A. Sefiani, A. Carrie, P. Billuart, N. McDonell, P. Couvert, F. Francis, P. Chafey, F. Fauchereau, G. Friocourt, V. des Portes, A. Cardona, S. Frints, A. Meindl, O. Brandau, N. Ronce, C. Moraine, H. van Bokhoven, H. H. Ropers, R. Sudbrak, A. Kahn, J. P. Fryns, R. Beldjord, and J. Chelly.** 2000. A new gene involved in X-linked mental retardation identified by analysis of an X;2 balanced translocation. Nat. Genet. **24:**167–170.